Transactions of the SMiRT 27
Yokohama, Japan, March 3-8, 2024
Division III

STUDY ON FLUID-STRUCTURE-SOIL-INTERACTION (FSSI) EFFECTS FOR A DEEPLY EMBEDDED NUCLEAR FACILITY WITH A LARGE-SIZE POOL UNDER SEVERE EARTHQUAKES. PART 1: LINEAR SSI

Yuki Sato[1], Dan M. Ghiocel[2], Shunji Kataoka[3], Suguru Sato[4], and Yasutomi Morimoto[5]

[1] Senior Project Engineer, JGC Corporation, Kanagawa, Japan (sato.yuuki@jgc.com)
[2] President, GP Technologies, Inc., New York, USA (dan.ghiocel@ghiocel-tech.com)
[3] Principal Engineer, JGC Corporation, Kanagawa, Japan (kataoka.shunji@jgc.com)
[4] Engineer, JGC Corporation, Kanagawa, Japan (sato.suguru@jgc.com)
[5] Senior Project Manager, JGC Corporation, Kanagawa, Japan (morimoto.yasutomi@jgc.com)

ABSTRACT

The paper investigates the effects of the Fluid-Structure-Soil-Interaction (FSSI) on the seismic linear response of a deeply embedded nuclear facility with a large-size water pool under severe earthquakes. For deeply embedded typical RC (Reinforced Concrete) shear wall nuclear building designs including large water pool, a reasonably accurate finite modeling of the fluid is required instead of the simpler Housner type lumped mass-spring models used in the past. The paper presents the verification of an alternative FSSI modeling options by efficiently combining the ACS SASSI special capabilities in Option AA-F (SSI run in ACS SASSI with fluid) or Option AA-R (SSI run in ANSYS). The proposed new method, which adopts the ANSYS FLUID80 fluid elements in ACS SASSI via the advanced Option AA-F, was verified by comparing the responses with those obtained from the precedent SSI analysis conducted in ANSYS via Option AA-R with FLUID80 and FLUID30 elements. As well, the FSSI analysis with proposed new method was applied to a building with large-size pool inside of the structure. The FSSI analysis confirmed the dynamic behavior of the pool water affecting the deformation of the structures by comparing with the same building model without pool water. The analysis results with proposed FSSI analysis method using ACS SASSI Option AA-F demonstrated the possibility of its practical use for the design of nuclear facilities.

1. INTRODUCTION

In the seismic design modelling for nuclear power plants (NPPs), how to model the fluid in SSCs has been discussed many times. As well, deeply embedded structures are usually required for NPPs. To date, since many types of NPPs tend to adopt massive water pools in the structures, more rational modelling methods have been desired in seismic analyses, in consideration of Soil-Structure-Interaction (SSI) effect. For instance, 3D finite element analysis incorporating FSSI effects using ANSYS has been performed (Azad et.al, 2019). In this ANSYS modelling, the pool water was modelled using acoustic elements, ANSYS FLUID30. By using ACS SASSI Option AA-R, the excavation condensed complex impedance matrix is defined as a frequency-dependent MATRIX50 super-element computed using the SASSI methodology in complex frequency, and then is transferred from ACS SASSI to ANSYS model.

In this paper, as an alternative approach, FSSI analysis method using ACS SASSI with ANSYS FLUID80 is proposed. The ANSYS FLUID80 substructure stiffness and mass matrices were automatically extracted and then added to the ACS SASSI SSI model using ACS SASSI Option AA-F. As a sample of nuclear related buildings, an SSI model with and without large-size water pool inside the building (hereinafter called "BLDG15 model") is used for the study analysis. The overview of BLDG15 model is shown in Figure 1. The water pool is located at the 2nd floor from the ground. Nodes 2143 and 874 are located at the bottom of the pool. Nodes 5359 and 5053 are located at the top of pool.

The material properties of BLDG15 model are shown in Table 1. The structure material is assumed as RC. The water in pool is assumed as ordinary water.

The generic seismic GRS input at ground surface in the horizontal and vertical directions is shown in Figure 2. This generic GRS is similar with the NuScale SMR CSDRS input anchored to a maximum ground acceleration of 0.50g for horizontal direction and 0.40g for vertical direction.

The generic site soil profile is described by a uniform deep soil deposit with an Vs of 800 m/s, Vp = 1,600m/s, unit weight of 20 KN/m^3 with a S and P wave damping of 2%. These soil properties were considered as the iterated soil properties for the study. To define the seismic motion input for the SSI analysis of the deeply embedded BLDG15 structure, the in-column or within motions at the foundation level (associated to FIRS) were determined for X, Y and Z directions. To do this the ACS SASSI SOIL module was run with the outcrop motion defined at foundation level as the user input, and the in-column motion at foundation level requested as the user output. The SOIL module uses SHAKE methodology for computing the in-column soil motions at different depths.

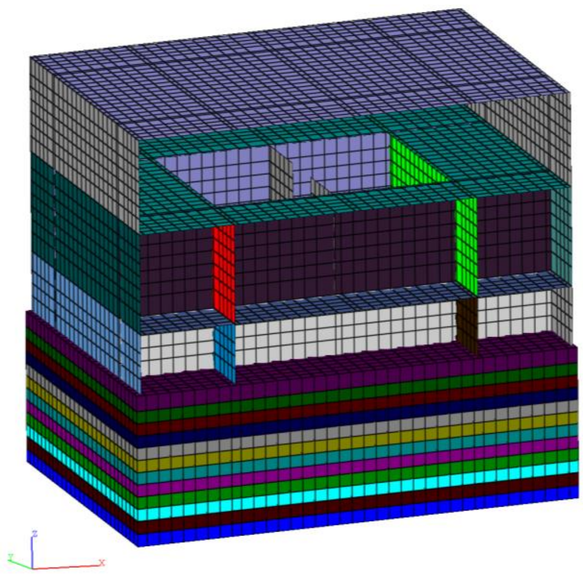

(a) SSI Model with Excavated Soil

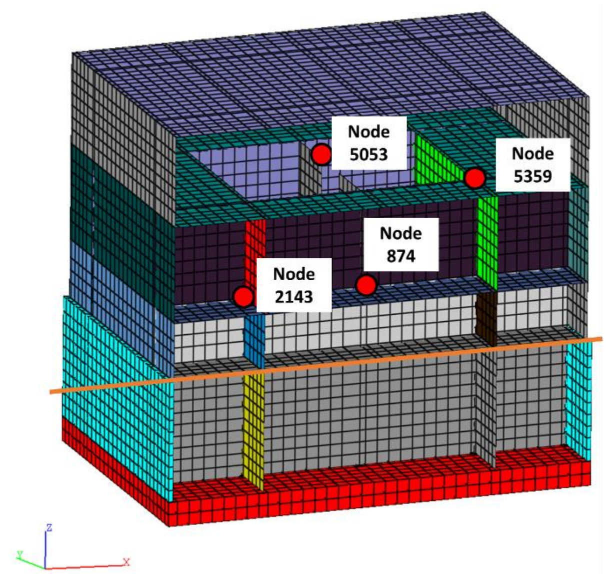

(b) SSI Model without Excavated Soil

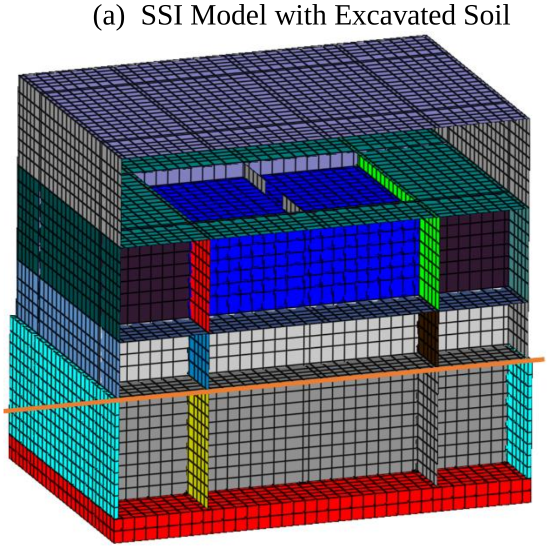

(c) SSI Model with Pool Water

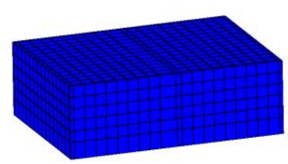

(d) Pool Water

Figure 1 BLDG15 SSI Model

Table 1 Material Property

Property	RC Structures (Basemat, Wall, Slab)	Pool Water
Unit Weight (kN/m^3)	23	10
Young's Modulus (kN/m^2)	2.57 x 10^7	-
Bulk Modulus (kN/m^3)	-	2.2 x 10^6
Poisson Ratio (-)	0.17	Approx. 0.5
Damping Ratio (%)	5	0.5

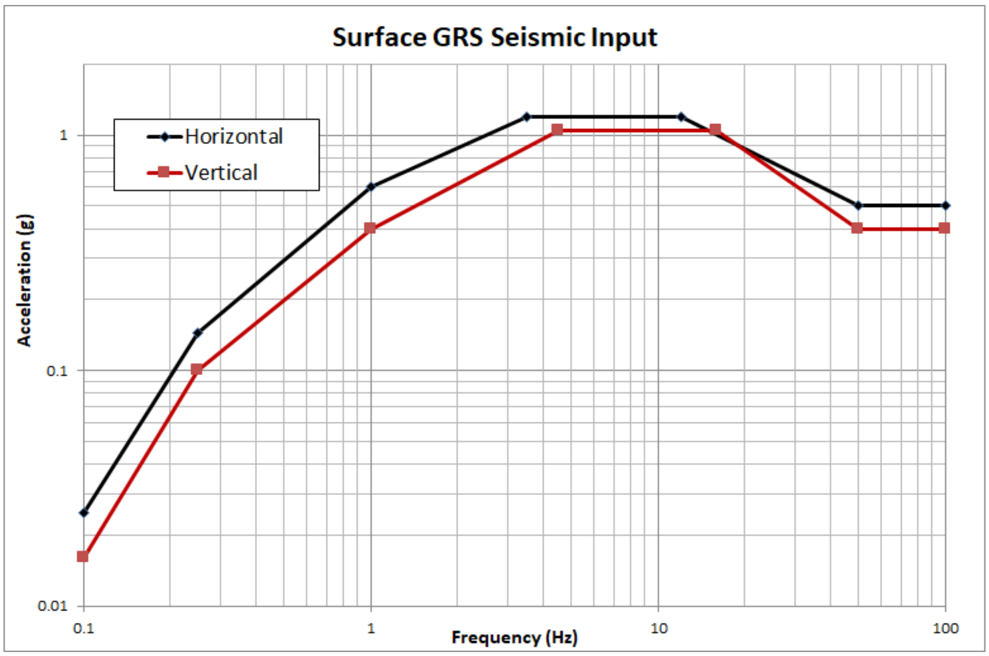

Figure 2 GRS Input for Horizontal and Vertical Direction for 0.50g Ground Acceleration

2. FAST SSI ANALYSIS OF DEEPLY EMBEDDED STRUCTURES

The ACS SASSI Flexible Volume Reduced-Order Modeling (FVROM) approach is a "theoretically exact" approach implemented in the ACS SASSI NQA software based on the condensation of the excavated soil impedance matrix at the foundation-soil interface nodes (Ghiocel, 2022).

The FVROM SSI approach uses the condensation of the excavated soil impedance matrix $\mathbf{Z}(\omega)$ at the foundation-soil interface nodes (the other excavation internal nodes and ground surface nodes are eliminated). The excavated soil matrix $\mathbf{Z}(\omega)$ is computed based on the the soil layering impedance matrix and the excavated soil dynamic matrix, i.e. $\mathbf{Z}(\omega) = \mathbf{X}(\omega) - \mathbf{C}^{e}(\omega)$ at each SSI frequency. The SSI system response is obtained using FVROM using the reduced-size excavated soil impedance matrix $\tilde{\mathbf{Z}}_{ii}(\omega)$ and the associated reduced-size load vector $\{\tilde{\mathbf{F}}_{i}(\omega)\}$ at each SSI frequency. The SSI system equation becomes for the reduced-size SSI system:

$$\begin{aligned} \left([\mathbf{C}_{ii}^{s}] + \tilde{\mathbf{Z}}_{ii}\right)\{\mathbf{U}_i\} + [\,\mathbf{C}_{is}^{s}]\{\mathbf{U}_s\} &= \{\tilde{\mathbf{F}}_i\} \\ [\mathbf{C}_{si}^{s}\,]\{\mathbf{U}_i\} + [\,\mathbf{C}_{ss}^{s}]\{\mathbf{U}_s\} &= \{\mathbf{0}\} \end{aligned} \tag{1}$$

where $[\mathbf{C}^s]$ and $\{\mathbf{U}_s\}$ are the structure dynamic stiffness and the complex displacement solution. Indices s and i correspond to structure and soil interface degrees of freedom, respectively.

The FVROM matrix condensation can be further combined with an efficient interpolation of the reduced-size soil impedance matrix in complex frequency. Such an approach which combines matrix condensation with fast interpolation is named FVROM-INT (FVROM with INTerpolation). Since the excavated soil impedance variation in frequency is much smoother than the SSI response variation, interpolating it is highly efficient for speeding up the overall computational effort of SSI analysis. Only a reduced number of frequencies can be used for accurately computing the condensed soil impedance matrix and seismic load vector, and then, interpolating them for the rest of all other SSI frequencies. For practical applications, for the FVROM-INT approach a reduced number of condensation frequencies of 15-25 are usually sufficient for an accurate interpolation of the soil impedance interpolation. After the SSI response is computed, say for 200-250 SSI frequencies, this response is further interpolated for all Fourier frequencies used for describing the input motion data in the frequency domain which may include 8,192, 16,384 or 32,768 Fourier frequencies, or even a larger number.

It should be noted that the FVROM-INT approach implementation can be used in conjunction with the “exact” FV method, but also other “approximate” methods as the different options of the Extended Subtraction Method (ESM) which are acceptable in practice. For latter case, the solution approximations inherent to the ESM method for the full-size SSI system are transmitted to the reduced-size SSI system. The FVROM-INT implementation has three computational steps:

1) *Identify key or condensation frequencies* based on free-field soil analysis results,
2) *Compute condensed excavation impedance matrices and seismic load vectors* for key frequencies to produce the frequency-dependent reduced impedance matrix and reduced load vector (for FVROM), and further *interpolate the reduced the excavation impedance matrix and seismic load vector* for all SSI frequencies (for FVROM-INT),
3) *Compute the SSI system solution* using the reduced excavated soil impedance matrices and seismic load vectors for all SSI frequencies.

3. FLUID MODELING FOR SEISMIC FSSI ANALYSIS

The ACS SASSI Option AA-F should be used to include pool fluid substructure. The fluid elements, which are the ANSYS FLUID80 elements, are extracted by specific automatic procedure. Using ACS SASSI UI ANSYS model converter, two FE models topologically identical to the ANSYS model including structure and fluid were generated for ACS SASSI. The ANSYS 8-node FLUID80 elements were converted to 8-node ACS SASSI SOLIDF elements These SOLIDF are “fake” SOLID elements, used as place holders for the FLUID80 substructure matrices inclusion, being used only for a model topology and equation mapping between the ANSYS and the ACS SASSI models.

The application of Option AA-F includes two stages:

Stage 1: *PREPARE ANSYS and ACS SASSI FSSI MODELS*: Prepare the ANSYS FSSI FE model including a single or multiple FLUID80 element substructures (such as pools or vessels), and then, convert this model into an ACS SASSI model with “fake” SOLIDF. Then, delete all the non-fluid elements to retain only the FLUID80 substructures for which the dynamic property matrices can be extracted and assembled with ACS SASSI model matrices using a specialized ANSYS macro (called "gen_fl80_kmc.mac"). This ACS SASSI FSSI model creation step is visually described in Figure 3.

Stage 2: *RUN ACS SASSI FSSI ANALYSIS:* Run FSSI analysis using the ACS SASSI FSSI model with the FILE80 substructure matrices integrated within the FSSI system matrices.

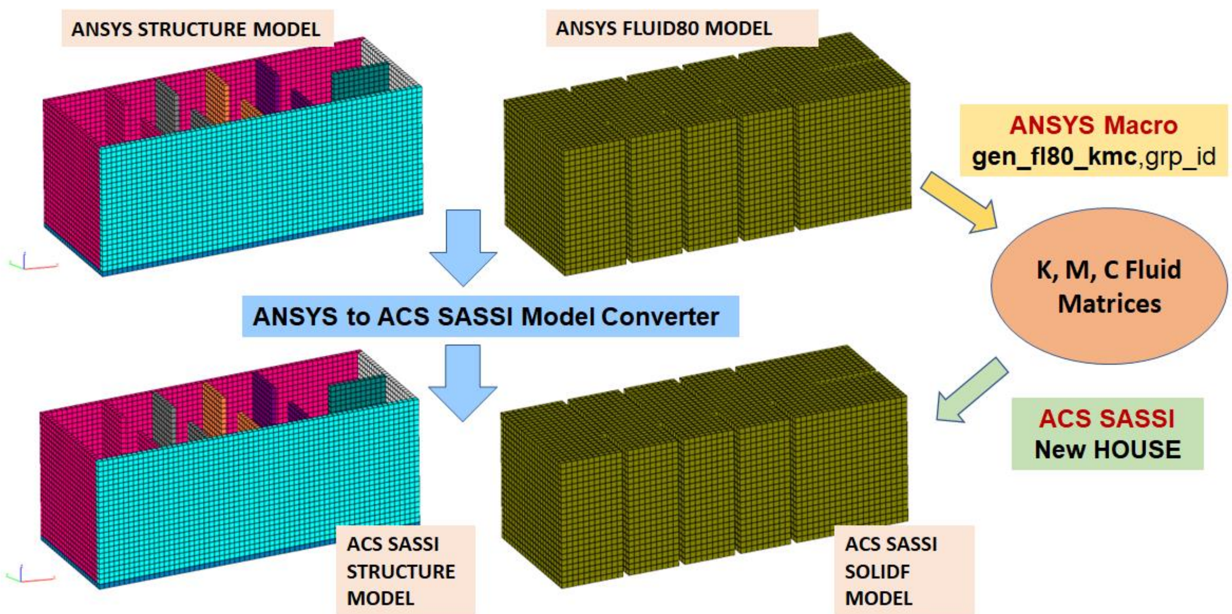

Figure 3. Description of the Option AA-F Procedure for Building ACS SASSI FSSI Model

4. VERIFICATION OF ANALYSYS MODELLING

As a verification of the modelling of ACS SASSI with FLUID80 elements, following analyses were performed using the simple pool box model shown in Figure 4.

- Case 1: FSSI analysis using ACS SASSI with FLUID80 elements.
- Case 2: FSSI analysis using ANSYS with FLUID80 elements.
- Case 3: FSSI analysis using ANSYS with FLUID30 elements.

Case 1 is the analysis method developed for ACS SASSI with Option AA-F. This option enables ACS SASSI to couple structure analysis with fluid super-elements calculated by ANSYS with FLUID80 element type. The FLUID80 can be calculated using the strain-stress relationship formulated as below;

$$\begin{Bmatrix} \varepsilon_{bulk} \\ \gamma_{xy} \\ \gamma_{yz} \\ \gamma_{zx} \\ R_x \\ R_y \\ R_z \end{Bmatrix} = \begin{bmatrix} 1/K & 0 & 0 & 0 & 0 & 0 & 0 \\ 0 & 1/S & 0 & 0 & 0 & 0 & 0 \\ 0 & 0 & 1/S & 0 & 0 & 0 & 0 \\ 0 & 0 & 0 & 1/S & 0 & 0 & 0 \\ 0 & 0 & 0 & 0 & 1/B & 0 & 0 \\ 0 & 0 & 0 & 0 & 0 & 1/B & 0 \\ 0 & 0 & 0 & 0 & 0 & 0 & 1/B \end{bmatrix} \begin{Bmatrix} P \\ \tau_{xy} \\ \tau_{yz} \\ \tau_{zx} \\ M_x \\ M_y \\ M_z \end{Bmatrix} \quad (2)$$

where

ε_{bulk}: Bulk strain of fluid
K: Bulk modulus of fluid
P: Pressure of fluid

γ_{ij}: Shear strain of fluid for ij plain
S: Shear modulus of fluid (assumed as $K \times 10^{-9}$)
τ_{ij}: Shear stress of fluid for ij plain
R_i: Rotation of fluid about axis i
B: Torsional stiffness of fluid for i direction (assumed as $K \times 10^{-9}$)
M_i: Twisting force of fluid about axis i

To conduct the verification of ACS SASSI with FLUID80 using Option AA-F, Case 2 adopts ACS SASSI Option AA-R with ANSYS with FLUID80 elements in the FSSI analysis. Also, to conduct the verification of fluid modelling method, Case 3 adopts Option AA-R with ANSYS with FLUID30 elements in the FSSI analysis. In the analysis with FLUID30 elements, harmonic analysis with acoustic elements is performed. The pressure of fluid obtained by acoustic wave equations. The pressure is applied as one of external forces in the structural analysis at the boundary of fluid. The pool box model shown in Figure 4 is applied to the verification of the analysis method. The material properties are shown in Table 2. The seismic input and soil parameter used for the pool box SSI model are the same as BLDG15 model. The embedment depth of the pool box structure is 3 m.

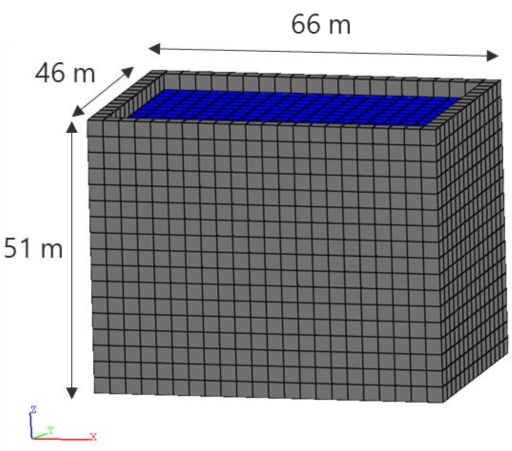

(a) Lateral view

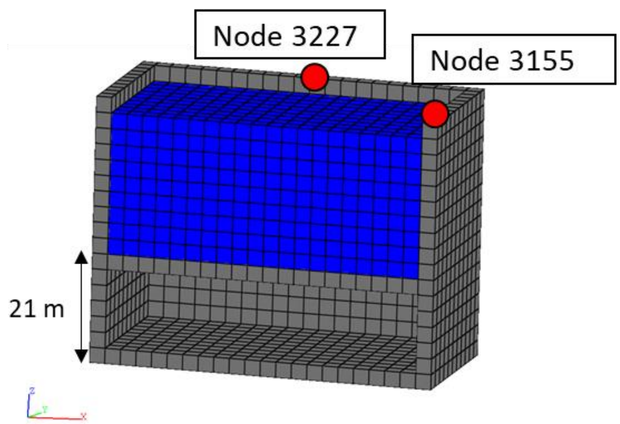

(b) Cross-section view

Figure 4 Overview of Pool Model

Table 2 Material Property of Pool Model

Object	Parameter	Value
Structure	Young's Modulus (GPa)	25.7
	Poisson Ratio (-)	0.17
	Density (kg/m^3)	2300
	Damping ratio (%)	5
Fluid	Bulk Modulus (GPa)	2.2
	Viscosity (Pa · s)	1.003×10^{-3}
	Density (kg/m^3)	1000

In-Structure Response Spectra (ISRS) of acceleration extracted on the position shown in Figure 4 were compared between Case 1, Case 2 and Case 3. The comparison results of ISRS are shown in Figure 5. The spectral shapes have good agreements among three cases. Although some differences of magnitude appear at the peak between ANSYS analysis with FLUID80 and ANSYS analysis with FLUID30, the global behaviors of the structures can be considered the same among all three cases. From this result, FSSI analyses for embedded structures using ACS SASSI with FLUID80 (via Option AA-F) can provide comparable results comparing with those using ANSYS with FLUID80/30 (via Option AA-R).

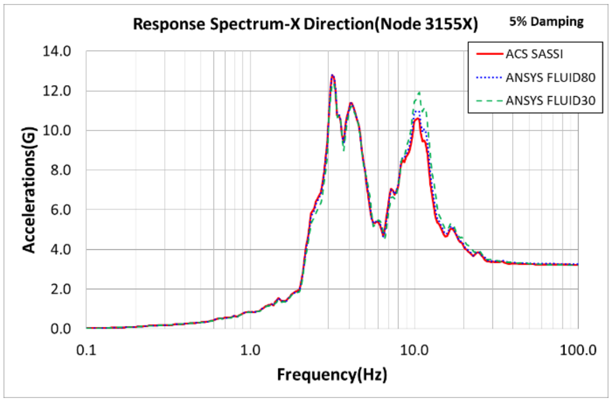

(a) Node 3155 in X direction

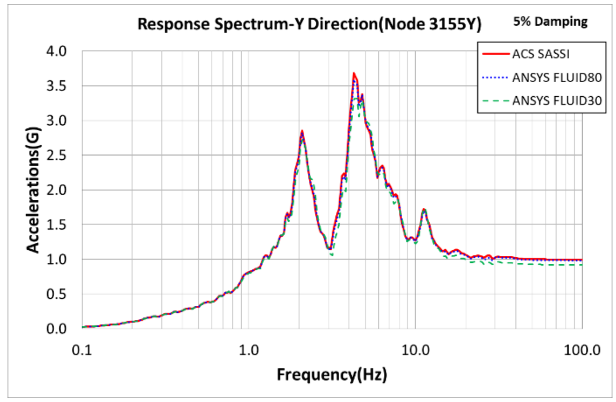

(b) Node 3155 in Y direction

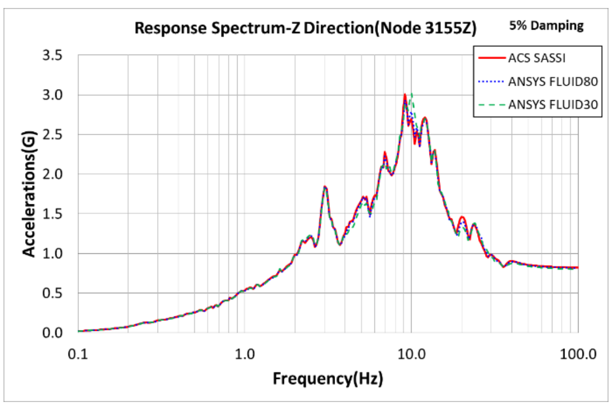

(d) Node 3155 in Z direction

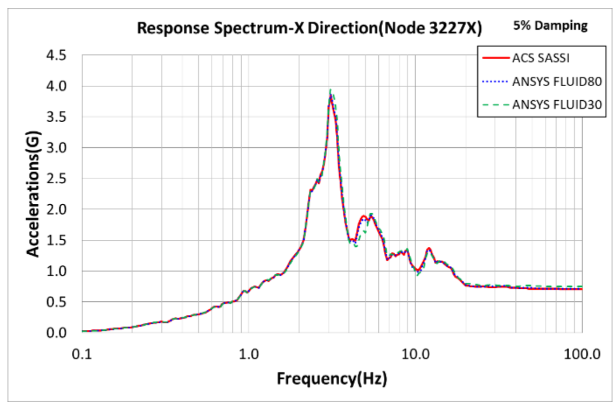

(d) Node 3227 in X direction

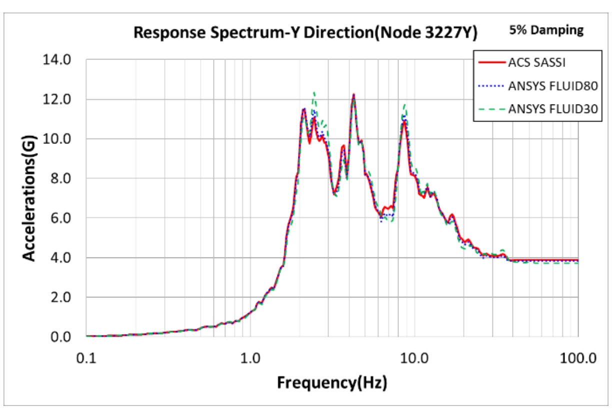

(e) Node 3227 in Y direction

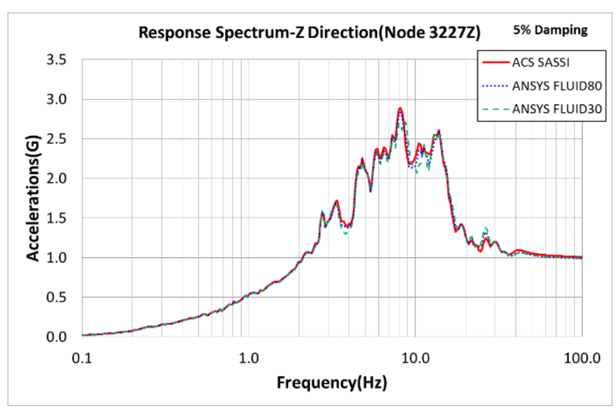

(f) Node 3227 in Z direction

Figure 5 ISRS at Top of Pool Wall in Pool Model

Maximum principal stresses in each direction extracted on the blue-highlighted element positions shown in Figure 7 were compared between Case 1, Case 2 and Case 3. The comparison results of maximum stress are also shown in Figure 7. The principal stresses have good agreements among three cases, although some small differences appear at the positions which have relatively high maximum stresses among three cases. One of major reasons for this phenomenon can be related to setting of damping ratio of fluid. In ACS SASSI method, the damping ratio of fluid was set to 0.5% as required by most of the engineering standards, including JEAC4601 and other international standards, however other methods treated the damping effect of fluid derived from the fluid viscosity.

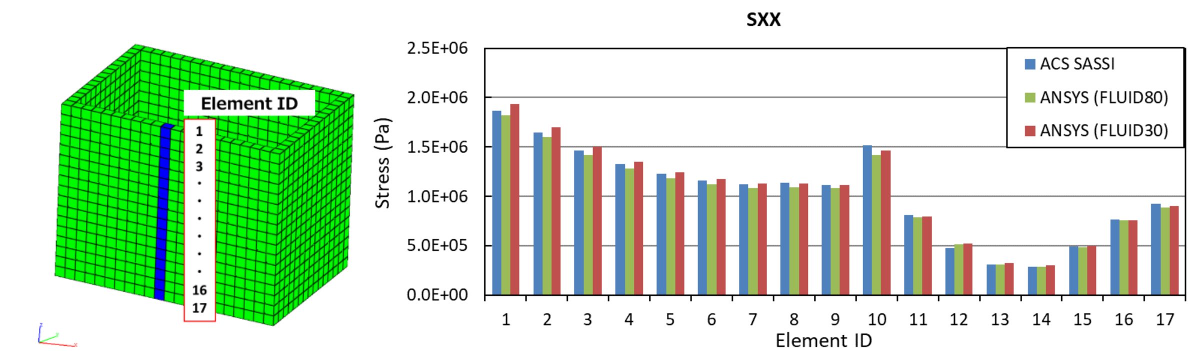

(a) Principal Stress in X direction

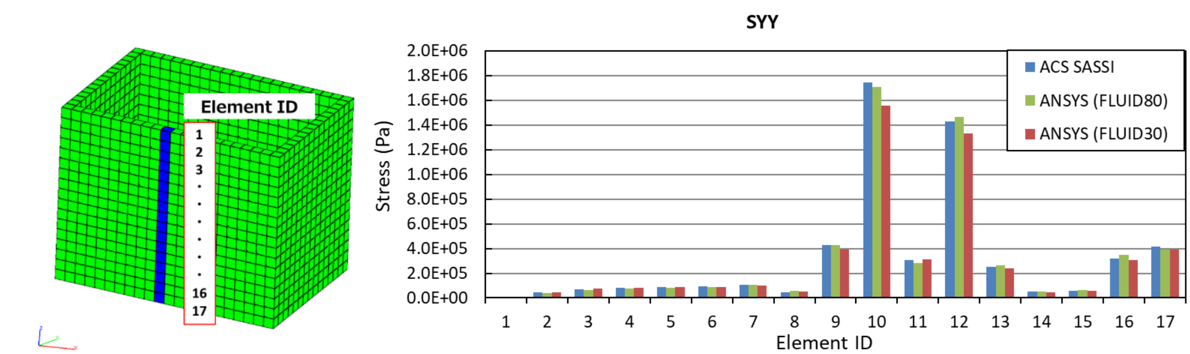

(b) Principal Stress in Y direction

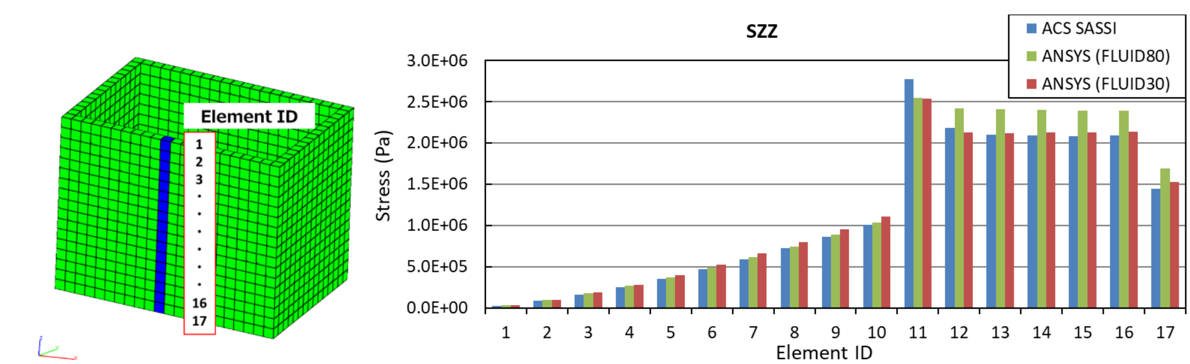

(c) Principal Stress in Z direction

Figure 7 Maximum Principal Stress for Pool Box Model

5. ANALYSIS RESULT FOR BLDG15 MODEL

In this section, the effect of pool water on the building structures is presented using ISRS and stress distribution. ISRS with and without fluid were compared as shown in Figure 8. As for Node 874, ISRS presents large difference of for horizontal direction, however some differences at higher frequency range appear for vertical direction. As for Node 5053 located at the top of internal wall inside of the pool, some significant difference appears for both horizontal and vertical directions. Especially for X direction, the peak of the acceleration was significantly shifted to lower frequency ranges because pool water behaved as additional mass of the internal wall by exerting the water pressure onto the internal walls.

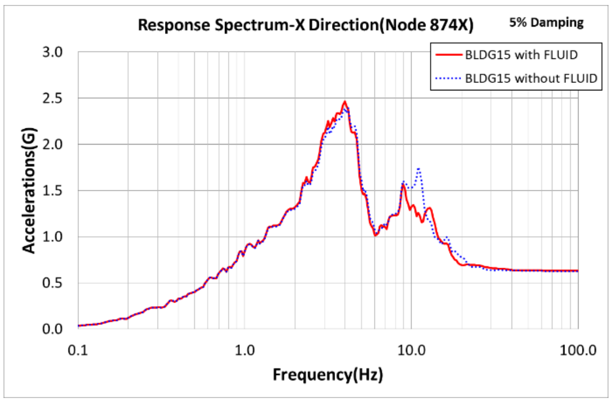

(a) Node 874 in X direction

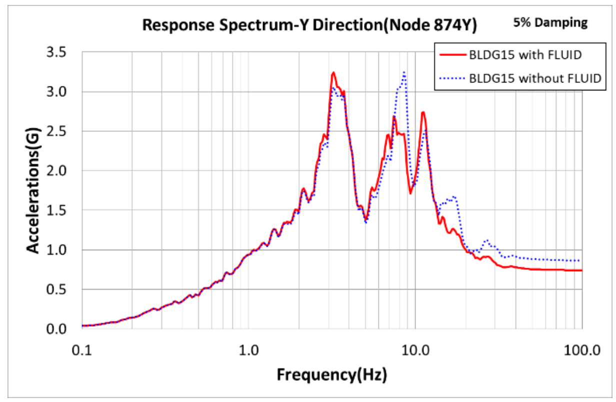

(b) Node 874 in Y direction

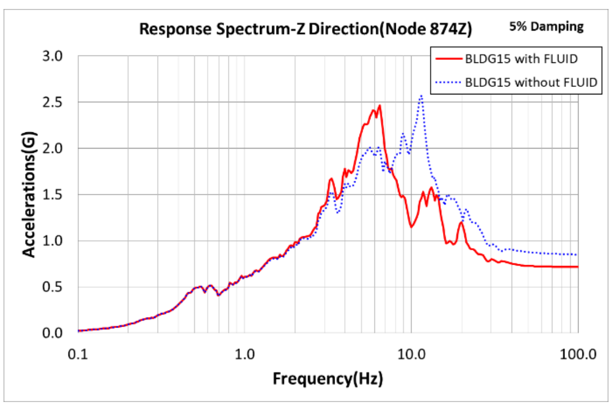

(c) Node 874 in Z direction

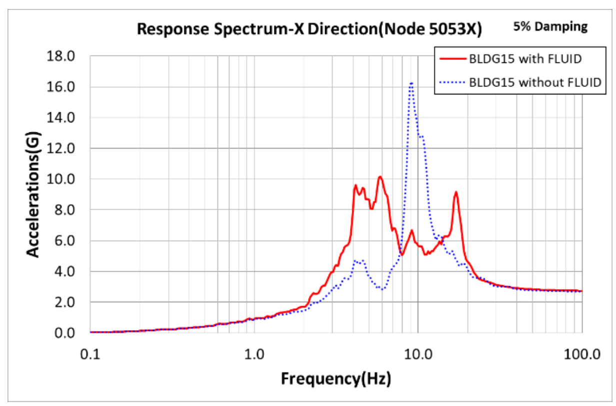

(d) Node 5053 in X direction

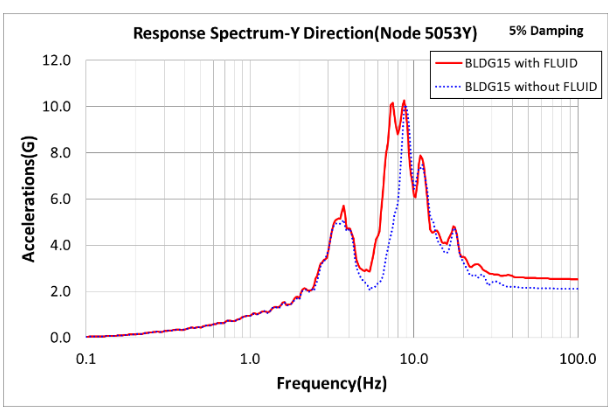

(e) Node 5053 in Y direction

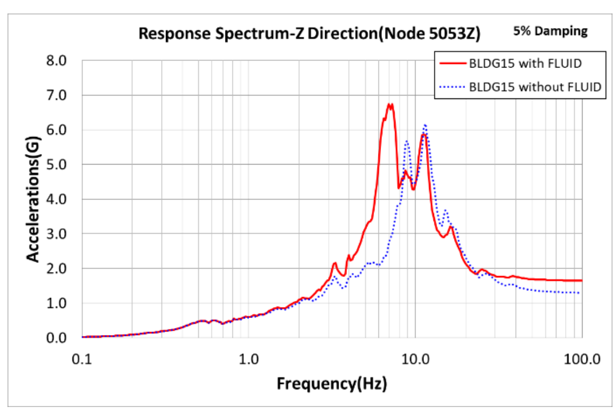

(f) Node 5053 in Z direction

Figure 8 ISRS in BLDG15

The stress distributions were compared for BLDG15 models with and without fluid. The positions of stresses extracted from lateral wall and internal wall are shown in Figure 9 and 10, respectively. The maximum stresses at the selected element positions are also shown in the figures.

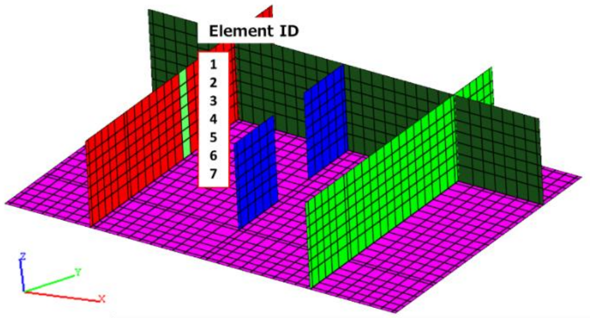

(a) Selected Position

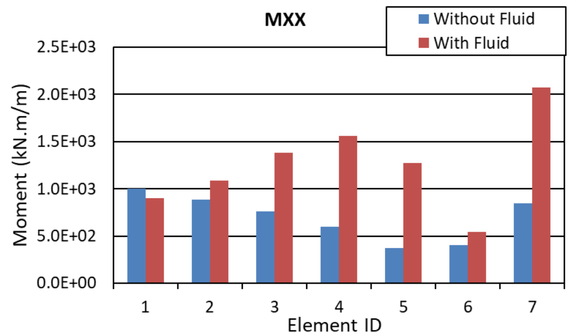

(b) Moment Mxx at Internal Wall

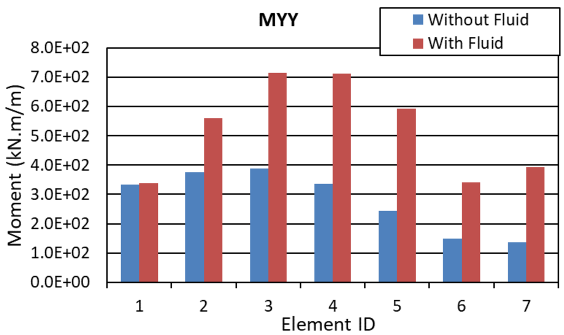

(c) Moment Myy at Internal Wall

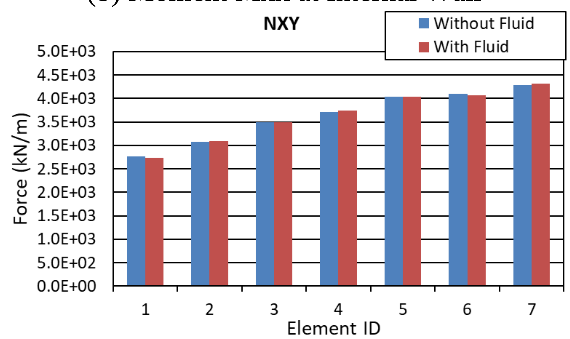

(d) In-Plane Shear Stress Nxy

Figure 9 Maximum Stress Distribution at Internal Wall

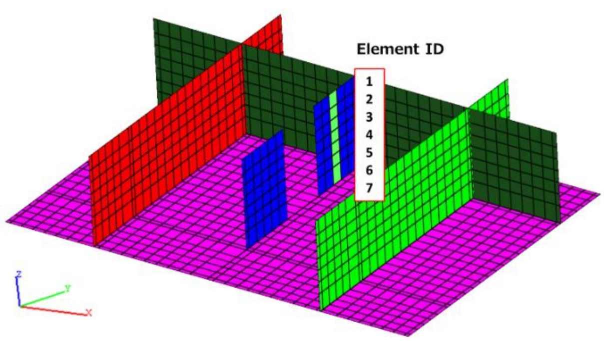

(a) Selected Position

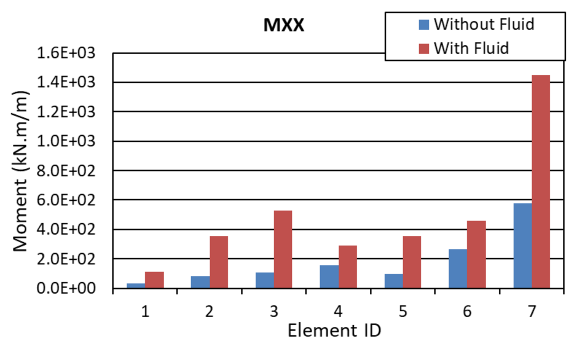

(b) Moment Mxx

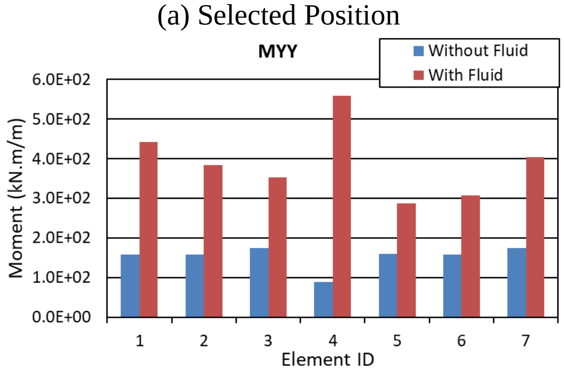

(c) Moment Myy

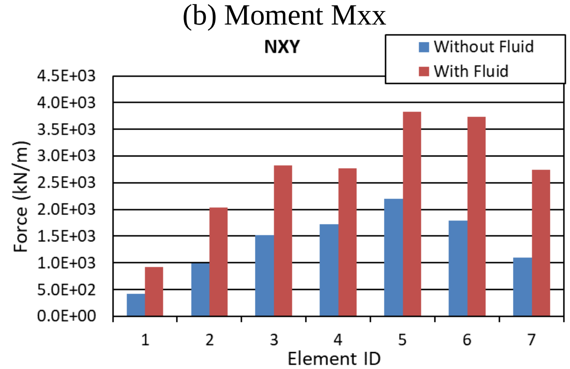

(d) In-Plane Shear Stress Nxy

Figure 10 Maximum Stress Distribution at Lateral Wall

For the lateral wall, there are significant differences of moments between with-fluid and without-fluid cases. With-fluid case has larger moments because of water pressure effects on the wall surface. As for in-plane shear stress for the lateral wall, there is no significant difference between two cases. This is because the water pressure mainly acts on the out-of-plane direction.

For the internal wall, there are significant differences of moments and in-plane shear stresses between with-fluid and without fluid cases. It can be observed that the free-edges of the internal walls augment the in-plane shear stress because water pressures are exerted on the wall in multiple directions.

6. CONCLUDING REMARKS

The paper investigates the fluid-structure-soil-interaction (FSSI) effects on the linear RC shear wall structure responses when subjected to a severe CSDRS earthquake motion with a 0.50g ground acceleration. From the verification study using embedded simple pool model, the analysis results clarified that FSSI analysis using ACS SASSI with FLUID80 (with Option AA-F) can provide close analysis results to the other fluid analysis solutions in ANSYS with FLUID80 or FLUID30 (with Option AA-R).

For the investigated BLDG15 case study, the computed SSI results show that even for a quite large water pool placed at a higher elevation, above at the second floor from the ground, the effects of the fluid-structure interaction were basically, localized around the pool, and only minimally transmitted to the rest of the structure responses.

Consequently, the FSSI analysis methodology using ACS SASSI Option AA-F has been established for the purpose of analyzing large-scale buildings. The more detailed application of this methodology will be investigated for envisioning practical designs of nuclear facilities.

7. REFERENCES

NuScale Power LLC., *NuScale Standard Plant Design Certification Application*, Revision 5, July 2020

Azad M., Brown N., Flores G. L. and Parker J. (2019), *3D Finite Element Modeling Approach for Seismic Analysis with Considerations of Small Modular Nuclear Reactors*, SMiRT25 Conference, Division 3, NC, USA, August 4-9.

Ghiocel, D.M, Nitta, Y., Ikeda, R. and Shono, T (2022). *Seismic Nonlinear SSI Approach Based on Best Practices in US and Japan. Parts 1: Modeling*, SMiRT26, Special Session on Nonlinear Seismic SSI Analysis Based on Best Practices in US and Japan, Berlin, July 10-15

Sato Y., Ghiocel D.M, Kataoka S., Sato S., and Morimoto Y. (2023). *Study on Fluid-Structure-Soil-Interaction (FSSI) Effects for A Deeply Embedded Nuclear Facility with A Large-Size Pool Under Severe Earthquakes. Part 2: Nonlinear SSI.* SMiRT27 Conference, Special Presentation Session Division 3, Yokohama, Japan, March 3-7

Japan Electric Association (JEA) (2017). "Technical Code for Seismic Design of Nuclear Power Plants JEAC4601-2015," JEA, Japan. [in Japanese].